Interchromophoric Interactions in Chiral X-type π-conjugated Oligomers: a Linear and Nonlinear Optical Study

David Cornelis[a], Edith Franz[b], Inge Asselberghs[b], Koen Clays[b], Thierry Verbiest[b], Guy Koeckelberghs[a,].*

Laboratory for Molecular Electronics and Photonics, Katholieke Universiteit Leuven, Celestijnenlaan 200F[a], 200D[b], B-3001 Leuven, Belgium.

guy.koeckelberghs@chem.kuleuven.be

RECEIVED DATE (to be automatically inserted after your manuscript is accepted if required according to the journal that you are submitting your paper to)

Abstract: A concept of chiral, X-type organized π-conjugated oligomers, linked by means of a binaphthalene pincer, is presented. NMR spectroscopy and cyclic and differential pulse voltammetry indicate that these oligomers are in close proximity and influence each other in a through-space manner in their neutral as well as in their oxidized states. The interaction between the oligomers was also confirmed by UV-vis, CD and emission spectroscopy. The synthetic versatility of this design also enables the development of hetero-coupled binaphthalene derivatives **BN1-2** and **BN1-3**, consisting of an electron-neutral oligothiophene or electron-rich oligomer and an electron-poor oligothiazole. Hyper-Rayleigh scattering data show a significant enhancement of the second-order nonlinear hyperpolarizability β for **BN1-3** and **BN1-2**, in contrast with the homo-coupled binaphthalene

derivatives (**BN1-1**, **BN2-2** and **BN3-3**). This enhancement provides direct proof for the through-space charge transfer interaction between the p-type and the n-type oligomer within **BN1-3** and **BN-1-2**.

Keywords: π-conjugated oligomers, binaphthalene derivatives, interchain interactions, hyper-Rayleigh scattering.

Introduction

During the last decade, the fundamental and applied research of π-conjugated systems has focused on the interplay between the intrinsic molecular features of the individual π-conjugated chains and their interchain interactions.[1] Some of these intermolecular couplings occur in the ground state, *e.g.* π-stacking;[2] others, such as exciton coupling,[3] arise in the excited state; in the oxidized state, the interchain hopping mechanisms contribute extensively to the electrical properties of these materials.[4]

To gain more fundamental insight into the origin and the strength of these interchain interactions, several oligomeric double-decker structures, constituted of two (stacked) oligothiophenes, have extensively been investigated.[5-7] Unambiguously, they gave evidence for the existence of interchain radical cation π-dimers. We recently implemented chirality by covalently linking two π-conjugated oligomers to a chiral binaphthalene unit in an overall X-type geometry.[8] This chiral X-type geometry was preferred, because it better ensures chiral exciton coupling between the two oligothiophene moieties, as previously demonstrated by CD experiments.[8] By further exploiting the chirality of the binaphthalene unit, we could qualitatively monitor the strength of any type of (induced) interchain interaction through chiroptical evaluation of the dihedral angle of the binaphthalene hinge.[9]

Perhaps the most compelling feature of π-conjugated systems as active elements in new generations of organic light-emitting diodes (oLEDs) and organic photovoltaic devices (oPVDs) comprises the charge transfer interaction between a p-type and a n-type π-conjugated system. Wang *et al.* studied the intermolecular charge transfer interaction by mixing an excess of *N,N*-dimethylaniline (p-type) with a series of distyrylbenzene derivatives (n-type) to invoke exciplex formation.[10] Alternatively, they

extensively investigated [2.2]paracyclophane-bridged distyrylbenzene systems containing donor and acceptor groups, and studied the impact of substitution patterns on their through-space interaction.[11]

We present a chirally linked p-type and n-type complex to model the charge transfer interaction of π-conjugated materials. This model compound (**BN1-3**) is constructed from an electron-rich morpholine-substituted oligothiophene and an electron-poor oligothiazole, which are covalently anchored by a chiral binaphthalene pincer (Figure 1). If through-space charge transfer occurs, this directly takes place between the two coupled oligomers, without any tunneling effects along a molecular bridge.

This manuscript first investigates the homo-coupled chiral X-type binaphthalene derivatives (**BN1-1**, **BN2-2** and **BN3-3**, Figure 1)). NMR spectroscopy and cyclic and differential pulse voltammetry are used to study the through-space π-electronic interactions between the oligomers in their neutral as well as in their oxidized states. Second, the **BNs** are evaluated by UV-vis, CD and emission spectroscopy in order to find *linear* optical evidence for a charge transfer interaction. On the basis of computational calculations on intermolecular electron donor-acceptor (EDA) complexes as potential high-efficiency second-order nonlinear optical materials,[12] all binaphthalene derivatives are finally analyzed by means of hyper-Rayleigh scattering to obtain additional *nonlinear* optical evidence for a through-space charge transfer process within **BN1-3** and **BN1-2**.

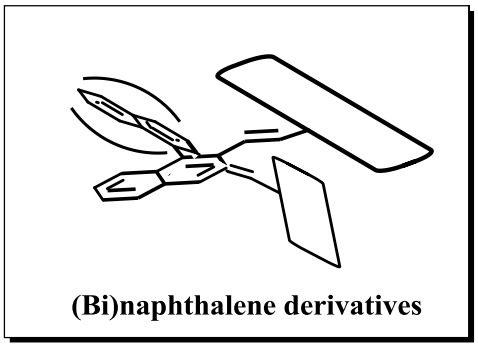

(Bi)naphthalene derivatives

Naphthalene derivatives

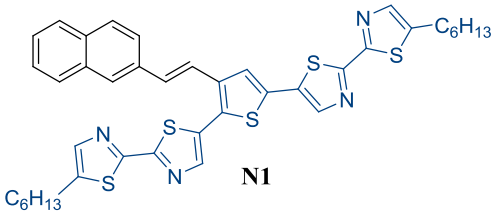

N1

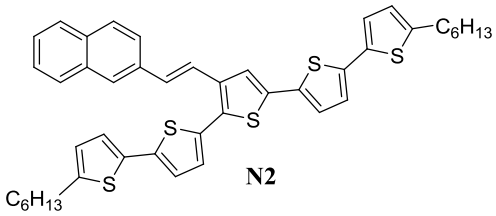

N2

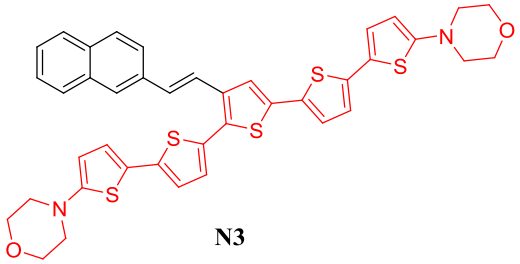

N3

Binaphthalene derivatives

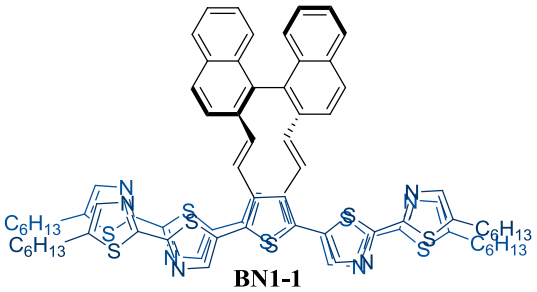

BN1-1

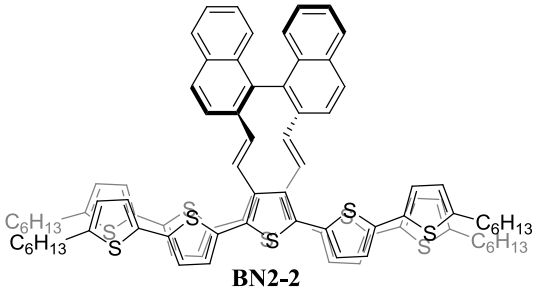

BN2-2

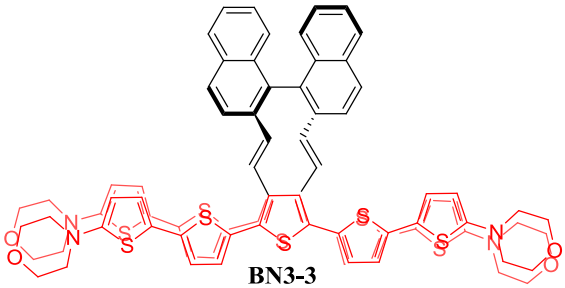

BN3-3

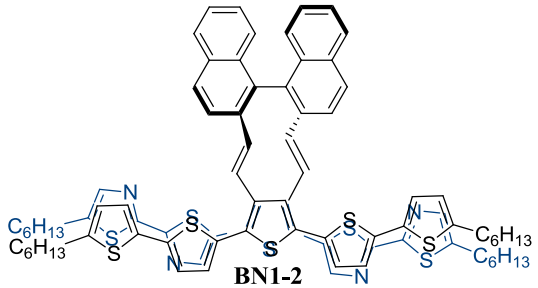

BN1-2

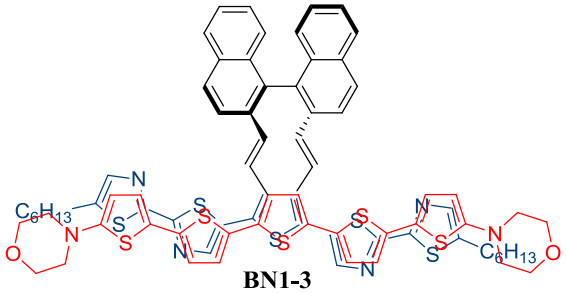

BN1-3

Figure 1. Overview of the synthesized (bi)naphthalene derivatives (**N1, N2, N3** and **BN1-1, BN2-2, BN3-3, BN1-2 and BN1-3**).

Experimental part

Reagents and instrumentation

All reagents were purchased from Aldrich Chemical Co. and Acros Organics and were used as received. Tetrahydrofuran (THF) was dried over a Na/K alloy. Dichloromethane, dimethylformamide (DMF) and hexane were freshly distilled and further dried on molecular sieve (4Å).

^{1}H and ^{13}C nuclear magnetic resonance (NMR) measurements were carried out with a Bruker Avance 300, 400 or 600 MHz apparatus. UV-Vis and emission spectra were recorded with a Varian Cary 400 and a PTI Photon Technology International apparatus respectively. The DSC measurements were performed on a Perkin-Elmer DSC 7 apparatus at the 2nd heating (heating rate = 40 °C/min). Cyclic and differential pulse voltammetry were performed on a Princeton Applied Research PARSTAT 2273, equipped with a standard three-electrode configuration. A Ag/AgCl (3M NaCl) electrode served as a reference electrode and a Pt wire and disk as the counter- and working electrode. The measurements were done in homogeneous solutions of ± 10^{-4} M binaphthalene derivative, 10^{-4} M ferrocene (internal standard) and 0.1 M Bu_4NBF_4 (supporting electrolyte) in dry dichloromethane under an argon atmosphere. The cyclic and differential pulse voltammograms were calibrated toward the Fe(II/III) couple at 0.60 V versus a standard calomel electrode.[13]

All samples are measured using the frequency resolved hyper-Rayleigh scattering technique as described before[14] with a Ti-sapphire laser (Spectra Physics). Crystal Violet (CV) dissolved in methanol was used as an octopolar external reference (β_{xxx} = 338 × 10^{-30} esu). All the samples were dissolved in chloroform. For each sample a concentration series is measured and compared with the reference series. Except for **BN1-2,** none of the samples showed interfering multi-photon fluorescence at the second-harmonic wavelength. **1**[9], **2**[9]**, *(S)*-5**[15], **6**[16], **11**[17], **BN2-2**[9], **BN1-2**[9], **13**[9] and **14**[9] were synthesized according to literature procedures.

Synthesis of 2-morpholine-5-tributyltinthiophene 7

A solution of **6** (1.05 mmol, 178 mg) in dry THF (4 mL) was purged with argon and cooled to -78 °C. Slowly, a solution of *t*-BuLi (1.11 mmol, 737 µL, 1.5 M in pentane) was added and the mixture was stirred for 20 min at -60 °C. Subsequently, a solution of tributyltin chloride (1.16 mmol, 377 mg) in dry THF (2 mL) was added and the reaction was allowed to reach room temperature. After 2 h of stirring at room temperature, the solvent was removed under reduced pressure and the product was redissolved in dry hexane. LiCl was filtered off and, after removal of the solvent, a brown oil was obtained, which was used in the next step without any further purification.

Yield: 430 mg (89 %).

^{1}H-NMR ($CDCl_3$; 300 MHz): δ = 6.85 (d, J = 3.7 Hz, 1H), 6.27 (d, J = 3.7 Hz, 1H), 3.84 (t, 4H), 3.15 (t, 4H), 1.55 (m, 6H), 1.32 (m, 6H), 1.05 (t, 6H), 0.89 (t, 9H).

Synthesis of 5-morpholine-[2,2'-bithiophene] 9

A solution of **7** (10.4 mmol, 4.74 g), **8** (15.5 mmol, 2.53 g) and $Pd(PPh_3)_4$ (260 µmol, 300 mg) in dry DMF (20 mL) was purged with argon and heated at 80 °C for 24 h. After reaction, the solvent was removed under reduced pressure and the product was extracted with chloroform. The combined organic layers were washed with a saturated KCl solution and dried over $MgSO_4$. The solvents were removed under reduced pressure and recrystallization of the crude compound from hexane afforded pure, pale yellow crystals.

Yield: 1.90 g (73 %).

m.p.: 125.9-126.2 °C.

^{1}H-NMR ($CDCl_3$; 300 MHz): δ = 7.10 (d, J = 4,8 Hz, 1H), 6.98 (dd, J = 4.8 Hz, J = 3.7 Hz, 1H), 6.95 (d, J = 3.7 Hz, 1H), 6.88 (d, J = 3.7 Hz, 1H), 6.05 (d, J = 3.7 Hz, 1H), 3.85 (t, 4H), 3.14 (t, 4H).

^{13}C-NMR ($CDCl_3$; 300 MHz): δ = 158.2, 138.3, 127.8, 124.5, 123.1, 123.0, 122.0, 106.0, 66.4, 51.5.

MS: m/z = 251 (M^+), 194 (M^+-C_4H_9) (calc.: 251.4).

Synthesis of 5-morpholine-5'-tributyltin-[2,2'-bithiophene] 10

The same procedure as described for the preparation of **7** was followed, starting from **9** (1.00 mmol, 251 mg). The crude oil was used in the next step without any purification.

Yield: 520 mg (96 %).

^{1}H-NMR (CD_2Cl_2; 300 MHz): δ = 7.09 (d, J = 3.7 Hz, 1H), 7.01 (d, J = 3.7 Hz, 1H), 6.86 (d, J = 4.0 Hz, 1H), 6.02 (d, J = 4.0 Hz, 1H), 3.80 (t, 4H), 3.11 (t, 4H), 1.56 (m, 6H), 1.34 (m, 6H), 1.10 (t, 6H), 0.90 (t, 9H).

^{13}C-NMR (CD_2Cl_2; 300 MHz): δ = 158.5, 143.8, 136.3, 135.0, 124.5, 123.2, 122.9, 105.7, 66.5, 51.6, 29.2, 27.6, 13.7, 11.1.

MS: m/z = 541 (M^+), 484 (M^+-C_4H_9) (calc.: 540.5).

Synthesis of 3

The same procedure as described for the preparation of **9** was followed, starting from **11** (260 μmol, 102 mg), **10** (911 μmol, 493 mg) and $Pd(PPh_3)_4$ (13.0 μmol, 15.0 mg) in dry DMF (3 mL). Recrystallization of the crude compound from isopropanol afforded a red solid.

Yield: 109 mg (57 %).

m.p.: 103.0-104.0 °C.

^{1}H-NMR (CD_2Cl_2; 300 MHz): δ = 7.19 (d, J = 3.7 Hz, 1H), 7.14 (s, 1H), 7.04 (d, J = 3.7 Hz, 1H), 6.95 (d, J= 3.7 Hz, 1H), 6.91 (d, J = 3.7 Hz, 1H), 6.90 (d, J = 3.7 Hz, 1H), 6.87 (d, J = 3.7 Hz, 1H), 6.04 (d, J = 3.7 Hz, 2H), 4.05 (qu, 4H), 3.80 (t, 8H), 3.27 (d, J = 21.9 Hz, 2H), 3.14 (t, 8H), 1.27 (t, 6H).

^{13}C-NMR (CD_2Cl_2; 300 MHz): δ = 159.1, 159.0, 139.3, 137.9, 135.6, 133.7, 131.9, 128.8, 128.7, 127.8, 126.8, 124.7, 123.7, 123.6, 123.3, 123.2, 122.3, 105.5, 66.4, 62.6, 51.4, 27.8, 16.5.

MS: m/z = 732 (M^+) (calc.: 733.0).

Synthesis of N1

A suspension of NaH (200 μmol, 4.80 mg), **4** (220 μmol, 34.4 mg) and **1** (200 μmol, 147 mg) in dry THF (5 mL) was purged with argon and vigorously stirred for 20 h at reflux temperature. After reaction,

the mixture was poured into a HCl solution (1 M) and extracted with dichloromethane. The combined organic layers were washed with a saturated NaCl solution and dried over $MgSO_4$. The solvents were removed under reduced pressure and the crude compound was further purified by column chromatography (silicagel, eluent: chloroform:hexane (5:5 v/v)). After cold trituration in methanol, a pure orange solid was isolated.

Yield: 147 mg (99 %).

m.p.: 182.8-183.5 °C.

^{1}H-NMR ($CDCl_3$; 400 MHz): δ = 7.94 (s, 2H), 7.78-7.88 (m, 4H), 7.70 (d, J = 8.6 Hz, 1H), 7.59 (s, 1H), 7.58 (s, 1H), 7.54 (s, 1H), 7.43-7.51 (m, 2H), 7.38 (d, J = 16.1 Hz, 1H), 7.24 (d, J = 16.1 Hz, 1H), 2.89 (t, 2H), 2.88 (t, 2H), 1.72 (m, 4H), 1.20-1.50 (m, 12H), 0.90 (t, 6H).

^{13}C-NMR ($CDCl_3$; 400 MHz): δ = 162.2, 161.0, 159.1, 143.4, 143.3, 142.4, 141.2, 140.2, 138.7, 134.2, 133.7, 133.4, 133.0, 132.6, 131.5, 128.7, 128.3, 127.9, 127.5, 126.6, 126.4, 124.9, 123.4, 120.5, 31.6, 28.8, 27.3, 22.7, 14.2.

MS (APCI): m/z = 737 (M^+) (calc.: 737.1).

Synthesis of N2

The same procedure as described for the preparation of **N1** was followed, starting from a suspension of NaH (141 μmol, 3.40 mg), **4** (141 μmol, 22.0 mg) and **2** (141 μmol, 103 mg) in dry THF (4 mL). The crude compound was further purified by column chromatography (silicagel, eluent: dichloromethane:ethylacetate (6:4 v/v)). After cold trituration in methanol, a pure orange solid was isolated.

Yield: 87.2 mg (84 %).

m.p.: 140.0-141.0 °C.

^{1}H-NMR (CD_2Cl_2; 400 MHz): δ = 7.78-7.88 (m, 4H), 7.71 (d, J = 8.6 Hz, 1H), 7.50 (d, J = 16.1 Hz, 1H), 7.46 (m, 2H), 7.44 (s, 1H), 7.19 (d, J = 16.1 Hz, 1H), 7.10 (s, 2H), 7.09 (d, J = 3.7 Hz, 1H), 7.04 (d, J = 3.7 Hz, 1H), 7.01 (d, J = 3.7 Hz, 2H), 6.71 (d, J = 3.7 Hz, 2H), 2.80 (t, 4H), 1.69 (qu, 4H), 1.20-1.50 (m, 12H), 0.91 (t, 6H).

^{13}C-NMR (CD_2Cl_2; 400 MHz): δ = 146.5, 146.4, 139.2, 137.7, 136.8, 135.9, 135.1, 134.9, 134.5, 134.4, 134.0, 133.6, 133.4, 131.8, 131.0, 128.6, 128.3, 127.9, 127.8, 127.0, 126.7, 126.3, 125.3, 125.2, 125.1, 124.0, 123.9, 123.7, 122.4, 122.1, 31.9, 30.5, 29.1, 22.9, 14.2.

MS (APCI): m/z = 733 (M^+) (calc.: 733.2).

Synthesis of N3

The same procedure as described for the preparation of **N1** was followed, starting from a suspension of NaH (139 μmol, 3.30 mg), **4** (153 μmol, 23.9 mg) and **3** (139 μmol, 102 mg) in dry THF (4 mL). The crude compound was further purified by column chromatography (silicagel, eluent: dichloromethane:ethylacetate (7:3 v/v)). After cold trituration in methanol, a pure red solid was isolated.

Yield: 93.5 mg (91 %).

m.p.: 220.0-221.0 °C.

^{1}H-NMR (THF-d_8; 400 MHz): δ = 7.90 (s, 1H), 7.77-7.86 (m, 3H), 7.75 (d, J = 8.8 Hz, 1H), 7.57 (s, 1H), 7.55 (d, J = 16.1 Hz, 1H), 7.37-7.47 (m, 2H), 7.34 (d, J = 16.1 Hz, 1H), 7.14 (d, J = 3.8 Hz, 1H), 7.12 (d, J = 3.8 Hz, 1H), 7.01 (d, J = 3.8 Hz, 1H), 6.97 (d, J = 3.8 Hz, 1H), 6.93 (d, J = 3.8 Hz, 1H), 6.92 (d, J = 3.8 Hz, 1H), 6.08 (d, J = 3.8 Hz, 2H), 3.75 (t, 8H), 3.11 (t, 8H).

^{13}C-NMR (THF-d_8; 400 MHz): δ = 159.9, 159.8, 140.4, 138.8, 137.3, 136.3, 135.9, 134.7, 134.1, 134.0, 132.6, 131.9, 131.6, 128.9, 128.6, 128.3, 128.2, 127.4, 126.8, 126.4, 125.5, 124.3, 124.1, 123.7, 123.5, 122.6, 122.5, 122.4, 105.9, 66.7, 51.9.

MS (APCI): m/z = No fragments observed.

Synthesis of 12 and BN1-1

The same procedure as described for the preparation of **N1** was followed, starting from a suspension of NaH (250 μmol, 6.00 mg), ***(S)*-5** (250 μmol, 77.6 mg) and **1** (250 μmol, 184 mg) in dry THF (5 mL). The mixture of mono- and disubstituted product (**12** respectively **BN1-1**) was separated and purified by column chromatography (silicagel, eluent: dichloromethane:ethylacetate (95:5 v/v)). Both derivatives were isolated as an orange solid.

Yield (**12**): 114 mg (51 %).

No melting point detected by optical microscopy or DSC below 250 °C.

Tg: 63.0 °C (determined by DSC at 2nd heating with a heating rate = 40 °C/min).

^{1}H-NMR (CD_2Cl_2; 300 MHz): δ = 9.59 (s, 1H), 8.17 (d, J = 9.1 Hz, 1H), 8.12 (d, J = 9.1 Hz, 1H), 7.90-8.09 (m, 4H), 7.79 (s, 1H), 7.71 (s, 1H), 7.61 (t, J = 8.6 Hz, 1H), 7.58 (s, 1H), 7.53 (s, 1H), 7.47 (t, J = 8.6 Hz, 1H), 7.20-7.40 (m, 4H), 7.00 (d, J = 8.6 Hz, 1H), 6.76 (s, 1H), 6.61 (d, J = 16.1 Hz, 1H), 2.87 (m, 4H), 1.69 (m, 4H), 1.20-1.50 (m, 12H), 0.89 (m, 6H).

^{13}C-NMR (CD_2Cl_2; 400 MHz): δ = 191.9, 162.4, 161.1, 159.2, 159.1, 143.7, 143.1, 142.7, 141.4, 141.3, 140.5, 138.5, 136.7, 135.0, 134.3, 133.3, 133.2, 133.0, 132.7, 131.8, 131.2, 130.1, 129.6, 129.5, 129.4, 128.9, 128.5, 127.7, 127.6, 127.5, 126.9, 126.8, 124.9, 123.2, 123.1, 122.5, 31.8, 29.0, 27.4, 22.9, 14.1.

MS (ESI): m/z = 1805 ($2M^+$ + Na) (calc.: 891.3).

Yield (**BN1-1**): 73.2 mg (20 %).

No melting point detected by optical microscopy or DSC below 250 °C.

Tg: 167.6 °C (determined by DSC at 2nd heating with a heating rate = 40 °C/min).

^{1}H-NMR (CD_2Cl_2; 600 MHz): δ = 8.05 (d, J = 8.6 Hz, 2H), 7.98 (d, J = 8.6 Hz, 2H), 7.96 (d, J = 8.6 Hz, 2H), 7.68 (s, 2H), 7.66 (s, 2H), 7.50 (s, 2H), 7.45 (t, J = 8.6 Hz, 2H), 7.41 (s, 2H), 7.25 (t, J = 8.6 Hz, 2H), 7.19 (d, J = 16.0 Hz, 2H), 7.10 (d, J = 8.6 Hz, 2H), 6.86 (s, 2H), 6.70 (d, J = 16.0 Hz, 2H), 2.84 (t, 4H), 2.79 (t, 4H), 1.69 (m, 8H), 1.20-1.50 (m, 24H), 0.90 (m, 12H).

^{13}C-NMR ($CDCl_3$; 300 MHz): δ = 162.0, 160.7, 159.2, 143.2, 143.0, 142.2, 141.1, 140.1, 138.8, 134.6, 134.0, 133.4, 133.3, 132.9, 132.6, 131.3, 131.1, 129.1, 128.3, 128.2, 127.1, 126.5, 125.0, 123.2, 122.3, 31.6, 28.8, 27.3, 22.7, 14.2.

MS (APCI): m/z = 1472 (M^+) (calc.: 1472.3).

Synthesis of BN1-3

The same procedure as described for the preparation of **N1** was followed, starting from a suspension of NaH (89.3 μmol, 2.10 mg), **12** (74.5 μmol, 66.4 mg) and **3** (89.3 μmol, 65.5 mg) in dry THF (4 mL). The crude compound was further purified by column chromatography (silicagel, eluent: dichloromethane:ethylacetate (9:1 v/v)). After cold trituration in methanol, a pure red solid was isolated.

Yield: 69.2 mg (63 %).

m.p.: 172.1 °C; Tg: 112.0 °C (determined by DSC at 2nd heating with a heating rate = 40 °C/min).

^{1}H-NMR (THF-d_8; 600 MHz): δ = 8.00-8.10 (m, 4H), 7.95 (d, J = 8.6 Hz, 1H), 7.94 (d, J = 8.6 Hz, 1H), 7.83 (s, 1H), 7.76 (s, 1H), 7.57 (s, 1H), 7.51 (s, 1H), 7.43 (t, J = 8.6 Hz, 1H), 7.39 (t, J = 8.6 Hz, 1H), 7.35 (d, J = 16.1 Hz, 1H), 7.26 (d, J = 16.1 Hz, 1H), 7.18-7.26 (m, 2H), 7.13 (d, J = 8.6 Hz, 1H), 7.09 (d, J = 8.6 Hz, 1H), 7.02 (s, 1H), 6.75-6.90 (m, 7H), 6.74 (s, 1H), 6.69 (d, J = 16.1 Hz, 1H), 6.03 (d, J = 3.7 Hz, 1H), 5.98 (d, J = 3.7 Hz, 1H), 3.73 (m, 8H), 3.08 (m, 8H), 2.88 (t, 2H), 2.87 (t, 2H), 1.69 (m, 4H), 1.20-1.50 (m, 12H), 0.90 (m, 6H).

^{13}C-NMR ($CDCl_3$; 600 MHz): δ = 161.9, 160.6, 159.3, 159.2, 158.6, 158.5, 143.1, 142.2, 141.1, 141.0, 140.1, 139.2, 138.8, 137.6, 136.4, 135.3, 134.9, 134.0, 133.9, 133.7, 133.6, 133.5, 133.4, 133.1, 133.0, 132.5, 131.8, 131.4, 131.3, 129.2, 129.0, 128.3, 127.4, 127.2, 127.0, 126.9, 126.4, 126.1, 125.0, 124.6, 124.0, 123.9, 123.7, 123.5, 123.4, 123.3, 122.3, 122.2, 122.1, 105.7, 100.1, 66.4, 51.3, 31.6, 28.8, 27.3, 22.7, 14.2.

MS (APCI): m/z = No fragments observed.

Synthesis of BN3-3

The same procedure as described for the preparation of **N1** was followed, starting from a suspension of NaH (136 μmol, 3.30 mg), ***(S)*-5** (63.5 μmol, 19.7 mg) and **3** (136 μmol, 100 mg) in dry THF (4 mL). The crude compound was further purified by cold trituration in methanol and isolated as a pure red solid.

Yield: 70.0 mg (75 %).

No melting point detected by optical microscopy or DSC below 250 °C.

Tg: 159.5 °C (determined by DSC at 2nd heating with a heating rate = 40 °C/min).

^{1}H-NMR (THF-d_8; 600 MHz): δ = 8.03 (s, 4H), 7.93 (d, J = 8.6 Hz, 2H), 7.40 (t, J = 8.6 Hz, 2H), 7.34 (d, J = 16.2 Hz, 2H), 7.21 (t, J = 8.6 Hz, 2H), 7.11 (d, J = 8.6 Hz, 2H), 6.88 (d, J = 3.7 Hz, 2H), 6.80-6.86 (m, 6H), 6.79 (d, J = 3.7 Hz, 2H), 6.77 (d, J = 3.7 Hz, 2H), 6.74 (s, 2H), 6.70 (d, J = 16.2 Hz, 2H), 6.02 (d, J = 3.7 Hz, 2H), 5.98 (d, J = 3.7 Hz, 2H), 3.72 (m, 16H), 3.07 (m, 16H).

^{13}C-NMR (THF-d_8; 400 MHz): δ = 159.9, 159.8, 140.2, 138.7, 137.3, 136.0, 135.6, 134.9, 134.3, 134.0, 133.8, 132.4, 132.2, 130.0, 129.3, 128.8, 128.3, 127.5, 127.2, 126.6, 125.3, 124.4, 124.2, 124.1, 124.0, 123.7, 123.6, 122.7, 122.5, 122.4, 105.9, 66.7, 51.8.

MS (APCI): m/z = No fragments observed

Results and discussion

Synthesis

The (bi)naphthalene derivatives **N1, N2, N3** (**BN1-1, BN2-2, BN3-3, BN-1-2** and **BN1-3)** are built up from the corresponding phosphonate-functionalized π-conjugated oligomers **1**, **2** or **3** and 2-naphthaldehyde **4** (respectively *(S)*-2,2'-diformyl-1,1'-binaphthalene ***(S)*-5**), as depicted in Scheme 1.

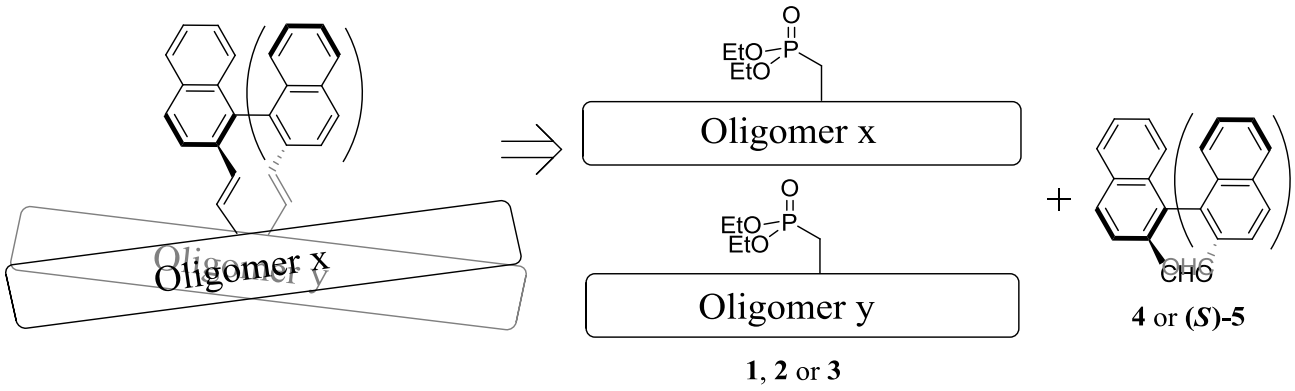

Scheme 1. Retrosynthesis of the (bi)naphthalene derivatives.

The synthesis of the electron-poor and the electron-neutral phosphonate **1** and **2** have already been reported.[9] The synthesis of the p-type phosphonate **3** is depicted in Scheme 2 and starts with the selective deprotonation and a subsequent stannylation of 2-morpholinethiophene (**6**) in the 5-position. It is worth noting that *t*-BuLi had to be used instead of *n*-BuLi to obtain a quantitative conversion and that the tributyltin functional group assured a better stability than the trimethyltin analogue. In this way, the stannylated product **7** was used without any purification in a Stille coupling with 2-bromothiophene (**8**) to expand the conjugated segment with an extra thiophene ring. For the stannylation of this morpholine-substituted bithiophene **9**, the same procedure was followed as for compound **7**. A final Stille coupling of the stannylated bithiophene **10** with the dibromo-functionalized phosphonate **11** afforded the p-type phosphonate **3**.

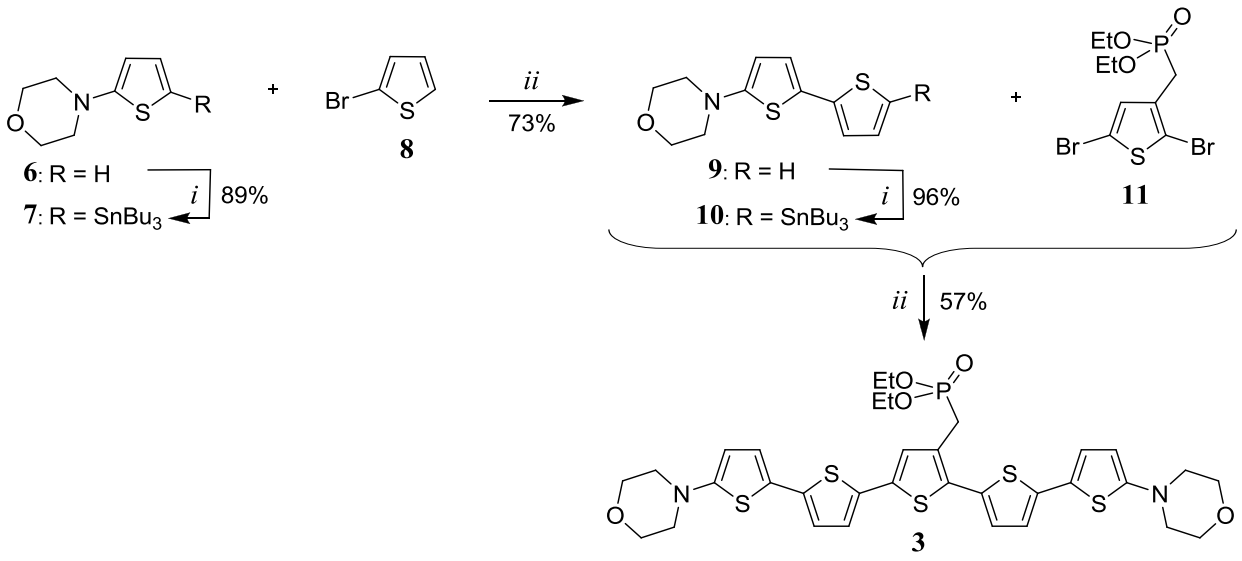

Scheme 2. Synthesis of the electron-rich phosphonate **3**. Conditions: *i)* 1) *t*-BuLi, THF, 2) Bu_3SnCl; *ii)* $Pd(PPh_3)_4$, DMF.

All three naphthalene derivatives **N1**, **N2** and **N3** were synthesized by means of a Wittig-Horner reaction of 2-naphthaldehyde (**4**) with the corresponding phosphonate (**1**, **2** or **3**) (Scheme 3). ^{1}H-NMR spectra unambiguously revealed an exclusive *trans*-configuration of the implemented double bond (see SI).

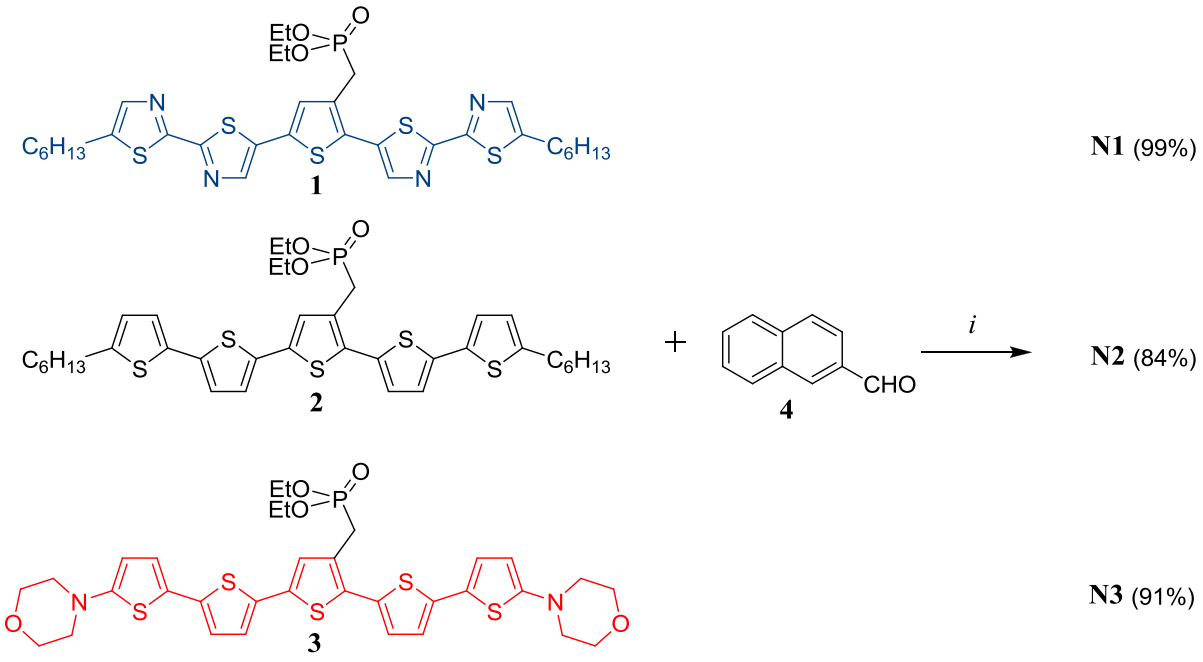

Scheme 3. Synthesis of the naphthalene derivatives (**N1-N3**). Conditions: *i)* NaH, THF.

The homo-coupled binaphthalene derivatives **BN1-1** and **BN3-3** were also prepared in a *trans*-selective configuration according to the same Wittig-Horner procedure (Scheme 4) as described for the naphthalene derivatives and similar to **BN2-2** and **BN1-2**.[9] The preparation of the hetero-coupled binaphthalene derivative **BN1-3** required the monosubstituted product **12**, which could be separated from **BN1-1** by means of column chromatography. A final Wittig-Horner reaction with phosphonate **3** afforded **BN1-3** in good yield.

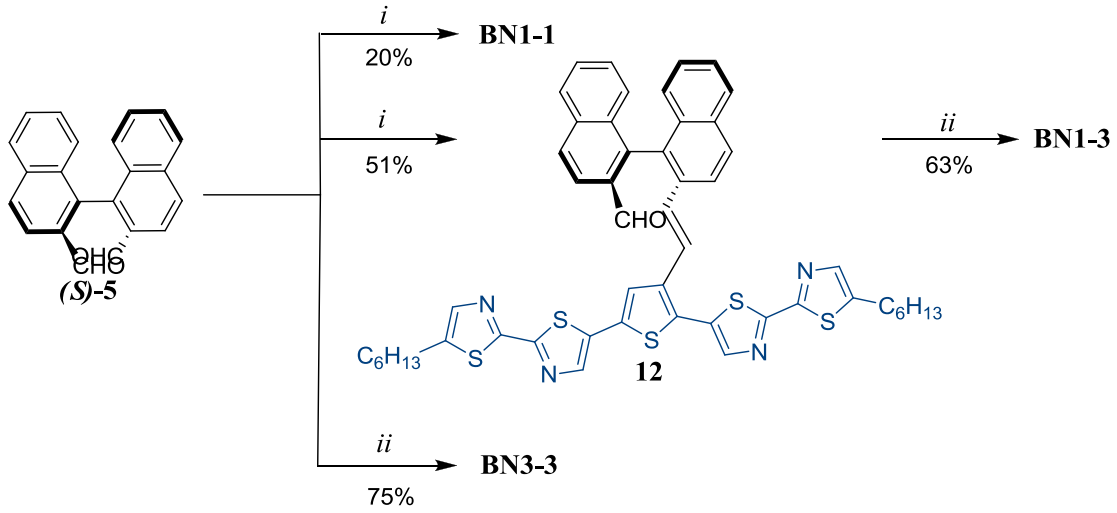

Scheme 4. Synthesis of the homo- and hetero-coupled binaphthalene derivatives **BN1-1**, **BN3-3** and **BN1-3**. Conditions: *i)* **1**, NaH, THF; *ii)* **3**, NaH, THF.

NMR analysis

By comparing the ^{1}H-NMR spectrum of **BN2-2** with those of two reference systems **13** and **14**, as depicted in Figure 2, possible interchain interactions between the two quinquethiophenes within **BN2-2** can elegantly be monitored. **13** consists of a single quinquethiophene, linked to a *t*-butyl group via a *trans* ethylene linker and **14** is the monosubstituted product in the Wittig-Horner reaction of ***(S)*-5** with **2**.

The aromatic region of the ^{1}H-spectrum of **BN2-2** (Figure 2.C) clearly shows that the spectrum is a superposition of two identical coupled 'naphthalene arms', which experience the same chemical environment as a result of a single conformation. Indeed, if both naphthalene arms would exhibit a different conformation, additional peaks would be expected in this region. A NOESY spectrum of **BN2-2** (SI) further reveals that this single conformation is characterized as drawn in Figure 2.C, *i.e.* the double bond proton **a** is oriented in such a way that it couples through space with the α-thiophene proton and the double bond proton **b** is in close proximity to the H3-proton of the naphthalene unit. Analogous ^{1}H-NMR patterns are found for **BN1-1** and **BN3-3**. However, the ^{1}H-spectra of **BN1-1** shows a small percentage (± 5 %) of an additional set of peaks due to an alternative, single conformation, which could not be unraveled in more detail.

Focusing on the oligomer protons of **13** and **14** learns that the outermost thiophene protons $\beta^{(')}$, $\gamma^{(')}$, $\delta^{(')}$ and $\varepsilon^{(')}$ (indicated in blue) resonate at more or less the same frequency. Only the innermost α-proton significantly differs due to the ring current effect of the adjacent naphthalene unit in **14**, which is absent in **13**. In comparison with the ^{1}H-spectrum of the homo-coupled **BN2-2**, a significant upfield shift can be observed for the outermost thiophene protons (marked in blue). This NMR shift gives evidence for a conformation in which both quinquethiophenes are in close proximity and influence each other through their individual aromatic ring current effect. Similar upfield shifts, also present when comparing the ^{1}H-NMR spectra of **N3** with **BN1-3** (SI), have been observed for stacked quinquethiophenophanes[5] and terthiophene-fused ketals.[6] The α-thiophene proton, on the other hand, undergoes a clear downfield shift with respect to **14**. The NMR signal is highly dependent on the ring current effect of the adjacent naphthalene ring. Because of the stacked conformation of **BN2-2**, the dihedral angle between the naphthalene moieties will be smaller in comparison with **14**[9] and thus also the ring current effect will change and give rise to a clear (downfield) NMR shift. Another proof of this difference in dihedral angle between **BN2-2** and **14** can be visualized by the NMR shift of the H8-proton of the binaphthalene unit. All naphthalene protons H1-7 of **14** and **BN2-2** (marked in red) resonate more or less at the same frequency. Only the H8-naphthalene proton of **BN2-2** exhibits a significant downfield shift with respect to **14**. The NMR signal for the H8-proton of **BN2-2** is also highly sensitive for the ring current effect of the adjacent naphthalene ring and alters with respect to **14** as a result of the attractive stacking interaction.[9]

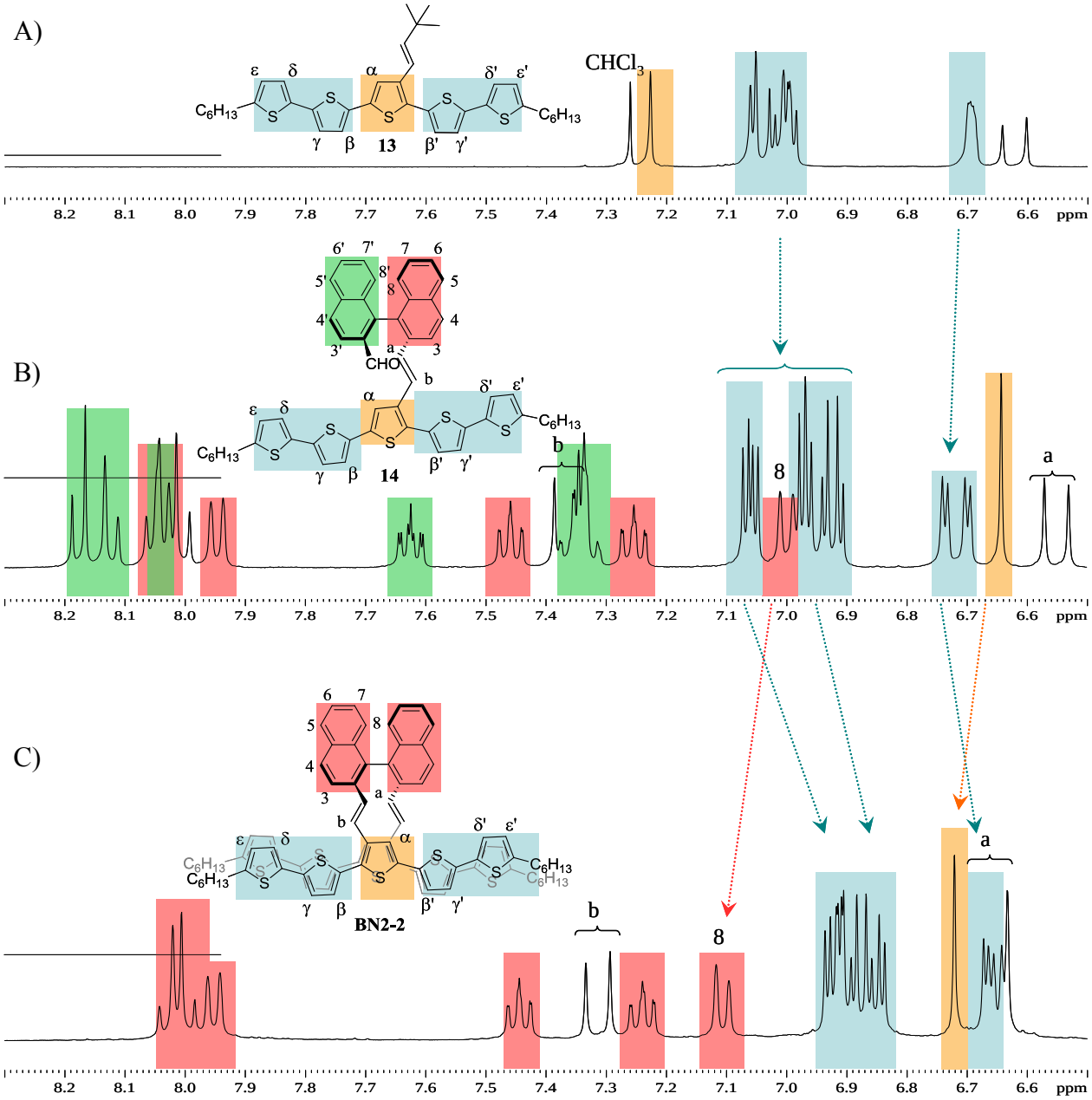

Figure 2. ^{1}H-NMR spectra of the aromatic region of A) **13** in $CDCl_3$, B) **14** and C) **BN2-2** in CD_2Cl_2.

In conclusion, the NMR analysis of **BN2-2** clearly demonstrates the potential of the binaphthalene unit as a suitable molecular pincer to interconnect two π-conjugated oligomers of similar bulkiness in a direct through-space manner.

Electrochemical analysis

In addition to the NMR analysis, the interchromophoric interactions within **BN2-2** can also be verified in the oxidized state. Therefore, the cyclic and differential pulse voltammograms of all compounds

studied are compared and depicted in Figure 3 (differential pulse voltammetry) and SI (cyclic voltammetry). **N2** and **BN2-2** show two quasi-reversible oxidations. For **N2**, this is consistent with a first one-electron oxidation, generating a radical-cation $\mathbf{[N2]^{+\cdot}}$ and a second one-electron oxidation affording the dication $\mathbf{[N2]^{2+}}$. In the case of **BN2-2**, no splitting of the first and second one-electron oxidation (generating $\mathbf{[BN2\text{-}2]^{+\cdot}}$ and $\mathbf{[BN2\text{-}2]^{2+}}$) can be observed and both oxidations occur at a lower potential than the unstacked analogue, as clearly shown in the differential pulse voltammogram in Figure 3a. This non-splitting and lowering of the oxidation potential is also found for Otsubo's quinquethiophenophanes[5], but contrasts with Collard's observation that the first oxidation peak of their stacked quinquethiophenes is split.[6] The fact that the first two one-electron oxidations of the stacked analogue take place at lower potentials than the one-electron oxidation of the linear analogue suggests that both $\mathbf{[BN2\text{-}2]^{+\cdot}}$ and $\mathbf{[BN2\text{-}2]^{2+}}$ are stabilized by an interaction between the oligothiophenes. The decrease of the potential of the first oxidation can be attributed to the stabilization of the radical-cation by the stacked, second oligothiophene, which already points to an interaction between the oligothiophenes. The non-splitting and the lowering of the second one-electron oxidation potential, generating $\mathbf{[BN2\text{-}2]^{2+}}$, shows that the stacked dication is stabilized in such a way that it overcomes the destabilization that might be expected from Coulombic repulsion. To unravel this stabilizing interaction in more detail, **BN2-2** was chemically oxidized in dichloromethane solution by means of a selective oxidant, Et_3OSbCl_6.[7,18] The gradual oxidation process was monitored with UV-vis and CD spectroscopy (see SI). These spectra readily revealed the formation of radical-cation π-dimers at higher oxidation level, visualized by the appearance of blue-shifted oxidation bands. Therefore, this additional stabilization of $[\mathbf{BN2\text{-}2}]^{2+}$ can clearly be attributed to π-dimerization.

At higher potential, the stacked analogue also undergoes subsequent oxidation, generating $[\mathbf{BN2\text{-}2}]^{3+}$ and possibly $[\mathbf{BN2\text{-}2}]^{4+}$. This latter process takes place without splitting and at higher potential than for the linear analogue, which may be ascribed to additional destabilization of the tricationic $[\mathbf{BN2\text{-}2}]^{3+}$ and the tetracationic $[\mathbf{BN2\text{-}2}]^{4+}$ through Coulombic repulsion.

An analogous behavior can be found for **N3** and **BN3-3** (although the oxidations occur at lower potentials), except that for **BN3-3**, the first (generating **[BN3-3]**$^{+\cdot}$) and second oxidation (to **[BN3-3]**$^{2+}$) are split. This can be explained by the fact that the π-dimerization in **[BN3-3]**$^{2+}$ cannot compensate for the strong stabilization of **[BN3-3]**$^{+\cdot}$ by the very electron-rich oligothiophenes.

For **N1** and **BN1-1**, finally, only an irreversible oxidation at much higher potentials is observed, which is in agreement with its electron-poverty. No reduction could be observed.

The voltammograms of the heterocoupled **BN1-2** and **BN1-3** are composed of an oxidation of the quinquethiophene or morpholine-substituted oligomer, an irreversible oxidation of the oligothiazole and possibly further oxidations to tricationic species. Compared with their homocoupled counterparts (**BN2-2** and **BN3-3**), the first oxidation of **BN1-2** and **BN1-3** occurs at a higher potential, showing that the oxidized quinquethiophene/morpholine-substituted oligomer is more stabilized by a pentathiophene/ morpholine-substituted oligomer than by the electron-poor oligothiazole.

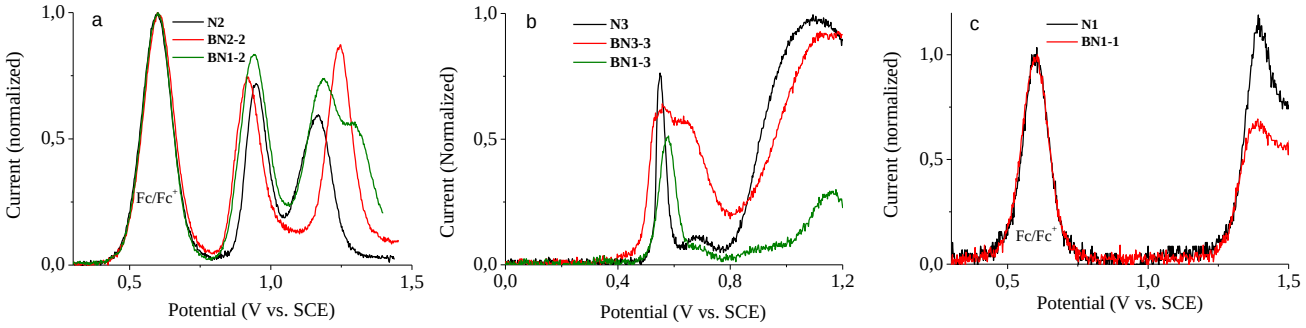

Figure 3. Normalized differential pulse voltammograms in dichloromethane with a pulse amplitude of 75 mV (50 ms) and a scan rate of 20 mV/s. Ferrocene was used as internal standard versus a standard calomel electrode[13]. In case a morpholine-substituted oligomer is present in the molecular structure, ferrocene was added after the measurement to avoid overlapping of the ferrocene signal.

In conclusion, this electrochemical study provides insight into the oxidation-induced interchain interactions between the coupled oligomers and reveals their interactions not only in the neutral but also in the oxidized states.

Linear optical properties

Our concept of (chirally) organizing two π-conjugated oligomers by means of a binaphthalene pincer in order to evoke interchain interaction in their neutral as well as in their oxidized states can also adequately be applied to study an interchromophoric charge transfer process. Therefore, hetero-coupled binaphthalene derivatives were developed **(BN1-3** and **BN1-2)**. **BN1-3** is particularly interesting, because it is constituted of an electron-rich morpholine-substituted oligothiophene (p-type) and an electron-poor oligothiazole (n-type).

To provide a baseline measure of the optical properties of the BN compounds, the absorption and emission spectra of both the BNs and the uncoupled naphthalene derivatives **N1-3** were considered (Figure 4). By focusing on the UV-vis spectrum of **BN1-3**, no significant characteristic (red-shifted) charge transfer absorption band can be observed. Further, the $\pi-\pi^*$ transition of **BN1-3** (around 418 nm) can almost fully be explained as a superposition of the spectra of **N1** and **N3** (see SI). These linear optical absorption spectra therefore show no direct proof for an intermolecular charge transfer complexation in the ground state. However, these data do not exclude the presence of a charge-transfer band, but they reveal that this band – if present – must be very weak.

The CD spectrum of **BN1-3** (Figure 4b) is a superposition of Cotton effects arising from the binaphthalene part and the two oligomers. However, while at $\lambda < 380$ nm the CD spectrum of such oligothiophene-substituted binaphthalene is constituted of Cotton effects arising from transitions located on the binaphthalene pincer and the oligomers, the CD spectrum $\lambda > 380$ nm solely originates from the oligomer's π-π* transition.[9] It is clear that in this region a bisignate Cotton effect is observed, which is fully in agreement with the theory of chiral exciton coupling. Therefore, this observation unambiguously demonstrates the chiral arrangement of the p-type and n-type oligomer.

All naphthalene compounds show a strong emission. The emission spectra of the homo-coupled BNs (Figure 4c) show a very similar shape as the constituting oligomers, demonstrating that the emission occurs from the oligomers. In the BN compounds, exciton coupling between the oligomers is present (see also the CD spectra). In such systems, the intensity of the fluorescence depends on the orientation of

the chromophores. In a cofacial arrangement, for instance, the fluorescence is quenched. Therefore, the somewhat lower intensity can be attributed to the exciton coupling, but due to the twisted orientation of the oligomers in the BNs, emission is still possible.

By comparing the emission spectrum of **BN1-3** with respect to **N1** and **N3** under the same conditions (chloroform, excitation at 375 nm), a total quenching of the fluorescence is observed for **BN1-3** in contrast to the uncoupled systems **N1** and **N3**. To account for the spectroscopic behavior of **BN1-3** and **BN1-2**, an excitation and emission process is outlined in Scheme 5. As already mentioned, the oscillator strength for the lower-lying intermolecular charge transfer excitation (process B) is considerably smaller than the A counterpart.[11b] Likewise, the radiative emission (the inverse process of B) has a low probability. After excitation, a rapid electron-transfer occurs. Subsequent nonradiative relaxation (process C) to the ground state results then in a full quenching of the fluorescence. This quenching of emission has also been observed by Bazan for the [2.2]paracyclophane derivative that consists of a cyclophane bridged donor-π-donor system with an acceptor-π-acceptor system[11b]. In **BN1-2**, finally, the emission is strongly reduced and originates from the **N2**-oligomer. This is perfectly in line with a slower electron transfer from **N2** to **N1** due to a smaller difference in electron-poverty, allowing the radiative emission from **N2** (the inverse process of A) to be competitive. It should, finally, be noted that energy- and electron transfer between orthogonal π-systems has been reported, leaving the possibility that energy is also transferred via the binaphthalene linker.[19]

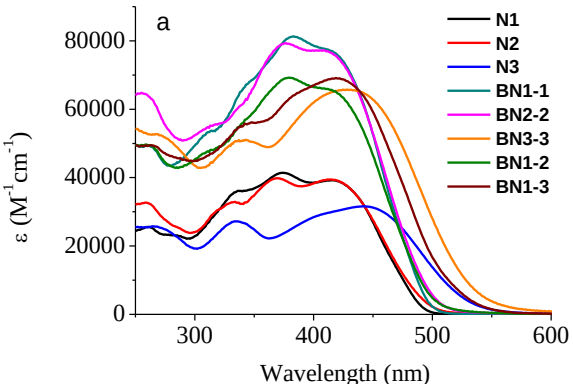

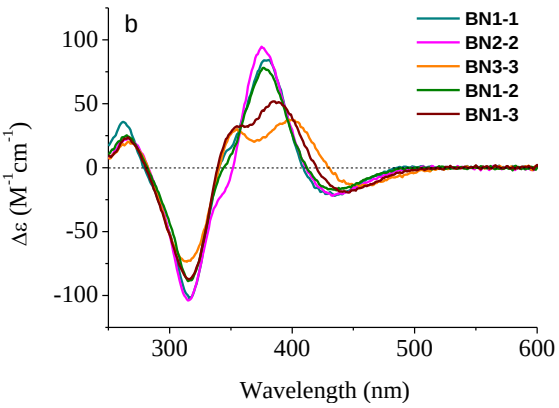

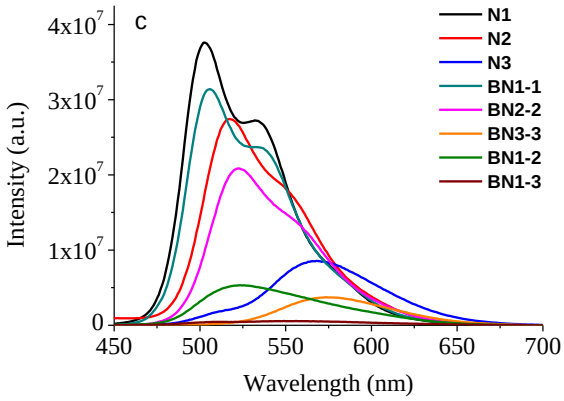

Figure 4: a) UV-vis spectra of **N1** (2.61×10^{-5} M), **N2** (2.67×10^{-5} M), **N3** (2.76×10^{-5} M), **BN1-1** (1.42×10^{-5} M), **BN2-2** (1.37×10^{-5} M), **BN3-3** (1.37×10^{-5} M), **BN1-2** (1.33×10^{-5} M) and **BN1-3** (1.34×10^{-5} M) in chloroform. b) CD spectra of **BN1-1** (1.42×10^{-5} M), **BN2-2** (1.37×10^{-5} M), **BN3-3** (1.37×10^{-5} M), **BN1-2** (1.33×10^{-5} M) and **BN1-3** (1.34×10^{-5} M) in chloroform and c) Absorption corrected emission spectra (excitation at 375 nm) of **N1** (1.31×10^{-6} M), **N2** (1.33×10^{-6} M), **N3** (1.38×10^{-6} M), **BN1-1** (7.09×10^{-7} M), **BN2-2** (6.86×10^{-7} M), **BN3-3** (6.83×10^{-7} M), **BN1-2** (6.66×10^{-7} M) and **BN1-3** (6.72×10^{-7} M) in chloroform.

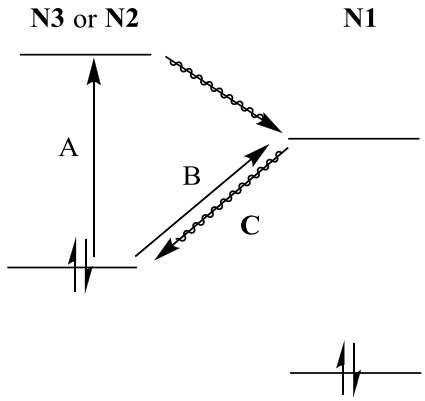

Scheme 5. Possible excitation and emission pathways, accounting for the spectroscopic behavior of **BN1-3 and BN-1-2**, shown for absorption of **N2**/**N3**.[11b]

Nonlinear optical properties

A charge-transfer interaction can also clearly be expressed by second-order nonlinear optical phenomena. Indeed, theoretical calculations have predicted a great enhancement of the second-order nonlinear hyperpolarizability β in intermolecular electron donor-acceptor complexes as a result of the large change in dipole moment that accompanies the charge-transfer and the relatively low-lying charge-transfer excitation energies.[12] As a consequence, the interaction between the electron-rich morpholine-substituted oligothiophene (p-type) and the electron-poor oligothiazole (n-type) in **BN1-3** should give rise to a significant enhanced second-order NLO response, which is not the case for the symmetrically substituted **BN1-1**, **BN2-2** and **BN3-3**. The same holds for **BN1-2**. Nevertheless, polar sandwich complexes have been studied and although the presence of a through-space interaction was confirmed by cyclic voltammetry, no second harmonic generation could be observed.[20]

The hyperpolarizabilities of **BN1-1**, **BN2-2**, **BN3-3** , **BN1-2** and **BN1-3** were determined by hyper-Rayleigh scattering (HRS). In classical 90° angle HRS geometry, the relation between β_{HRS} and the individual molecular tensor elements β_{ijk} is expressed as follows[21]:

$$\left\langle \beta_{ZZZ}^2 \right\rangle = \frac{1}{7}\sum_i \beta_{iii}^2 + \frac{6}{35}\sum_{i\neq j} \beta_{iii}\beta_{ijj} + \frac{9}{35}\sum_{i\neq j} \beta_{iij}^2 + \frac{6}{35}\sum_{ijk,cyclic} \beta_{iij}\beta_{jkk} + \frac{12}{35}\beta_{ijk}^2 \qquad \text{eq.1}$$

$$\left\langle \beta_{XZZ}^2 \right\rangle = \frac{1}{35}\sum_i \beta_{iii}^2 - \frac{2}{105}\sum_{i\neq j} \beta_{iii}\beta_{ijj} + \frac{11}{105}\sum_{i\neq j} \beta_{iij}^2 - \frac{2}{105}\sum_{ijk,cyclic} \beta_{iij}\beta_{jkk} + \frac{8}{35}\beta_{ijk}^2 \qquad \text{eq. 2}$$

Where the β_{IZZ} (I= horizontal(X) or vertical (Z) polarized second-harmonic light) is expressed at the macroscopic level and β_{ijk} at the molecular level. The overall measured hyperpolarizability β_{HRS} equals:

$$\beta_{HRS} = \sqrt{\langle \beta_{ZZZ}^2 \rangle + \langle \beta_{XZZ}^2 \rangle} \qquad \text{eq. 3}$$

In general, the HRS-response (β_{HRS}) of a molecule depends on both the electronic features and its symmetry. While the first parameter governs the magnitude of the individual tensor components β_{ijk}, the symmetry determines the relative contribution of the individual tensor components to the overall signal. Since the binaphthalene compounds are characterized by several transitions and since the symmetry clearly differs from the geometry typically found in π–systems endcapped with an electron-donating and -accepting group (DπA structures), the relative contribution of each individual tensor component cannot be derived from the HRS results only in a straightforward manner. However, since all four binaphthalene derivatives have the same shape, a comparison of the β_{HRS}-values does reveal possible electronic differences. The fact that the shape of each molecule is similar - the only difference is the heterocoupling instead of the homocoupling - is also in line with the fact that all compounds show similar depolarization ratios (ρ, expressed as $\rho = \langle \beta_{zzz}^2 \rangle / \langle \beta_{xzz}^2 \rangle$) (Figure 5). It must be mentioned that the experimental observation of statistically identical depolarization ratios for all BNs does not rule out a dipolar symmetry in the hetero-coupled **BN1-3** and **BN1-2**. Indeed, octopoles show the specific value of around 1.5, which can however also be found in dipoles for a particular hyperpolarizability tensor element combination, e.g. $\beta_{xzz} = -\beta_{zzz}$, all other tensor elements being zero. In general, a value for the depolarization ratio close to 1.5 makes it very difficult to correlate it with a particular symmetry. In principle, one expects an octopolar symmetry (T_d, D_{3h}, …), but a dipolar contribution can give values close to 1.5 as well.[22]

The static $\beta_{HRS}(0)$-values of the binaphthalene compounds, calculated using the two-level model including damping,[23] are displayed in Figure 5, from which two conclusions can be drawn: (i) within the experimental error, the homo-coupled **BN1-1**, **BN2-2** and **BN3-3** all exhibit a similar, nonvanishing

β_{HRS}-value, and (ii) the hetero-coupled **BN1-3** and **BN1-2** clearly show an increased HRS-response. Concerning the first observation, the noncentrosymmetry of the binaphthalene molecules accounts for the nonvanishing HRS response, which originates from octopolar contributions. More importantly, the increase in β_{HRS}-value of **BN1-3** can only be explained by the charge-transfer interaction between the two oligomers. Therefore, these observations provide direct proof for the interaction between the electron-rich oligothiophene and the electron-poor oligothiazole.[24]

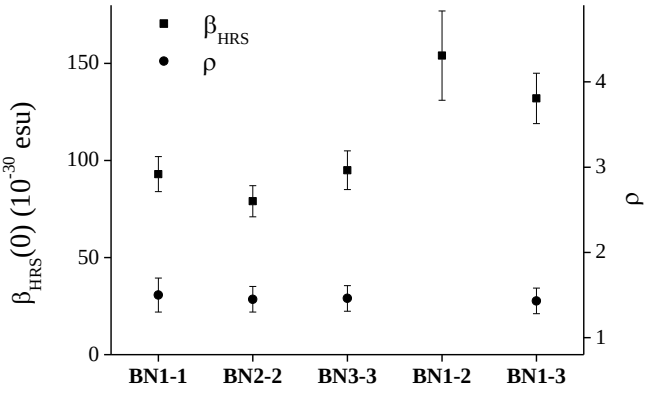

Figure 5. Static β_{HRS}-values of the homo-coupled **BN1-1**, **BN2-2** and **BN3-3** and the hetero-coupled **BN1-3** and **BN1-2** in chloroform solution and the depolarization ratios (excited at 880 nm). Since the HRS signal of **BN1-2** was contaminated with fluorescence, the high-frequency demodulation technique was applied to obtain a fluorescence free hyperpolarizability. Unfortunately, in these conditions the fluorescence free depolarization ratio could not be calculated. This also explains the higher experimental error of $\beta_{HRS}(0)$.

The sensitivity of the HRS technique for the charge transfer interaction can be correlated with equations 4 and 5:[25]

$$\alpha \propto \frac{M^2}{E} \qquad \text{eq. 4}$$

$$\beta \propto \frac{M^2 \Delta\mu}{E} \qquad \text{eq. 5}$$

in which M is the oscillator strength, E the energy difference between ground and excited state and $\Delta\mu$ the difference in dipole moment between ground and excited state. The transition studied is in fact the transition B in Scheme 5. From the UV-vis spectra, it is clear that M is rather small for this transition. However, the large change in dipole moment that accompanies the charge-transfer results in a significant $\Delta\mu$, increasing the sensitivity of the HRS technique for such transitions. It should be noted that since $\Delta\mu = 0$ for the transition between the stacked oligomers in the homo-coupled binaphthalene compounds, this transition cannot contribute to the overall HRS response in these molecules, making this contribution unique to hetero-coupled binaphthalene compounds. As a consequence, the combination of the high sensitivity and the selectivity for charge-transfer interactions renders HRS a particularly interesting technique to monitor such interactions. It should moreover be noticed that this observation provides, to the best of our knowledge, the first example of a HRS response originating from through-space charge transfer interactions, consistent with earlier published, computational data with respect to the role of intermolecular interactions within donor/acceptor π-electron chromophore molecules.[12]

Conclusions

In this work, we have described the synthesis and the properties of a series of chiral X-type binaphthalene derivatives (**BN1-1, BN2-2, BN3-3, BN1-2** and **BN1-3**) as suitable model compounds to monitor different types of (induced) interchain interactions between two π-conjugated oligomers. NMR spectroscopic studies on **BN2-2** have shown that the binaphthalene-linked quinquethiophenes influence each other through ring current effects, unequivocally indicating their close proximity due to attractive π-interactions. Electronic spectral and voltammetric measurements have revealed that the two stacked quinquethiophenes of **BN2-2** undergo delocalization in the first one-electron oxidation state and π-dimeric interactions in the second one-electron oxidation state. This evidence confirms the role of the binaphthalene unit as a suitable pincer molecule to interconnect two π-conjugated oligomers of similar bulkiness in a direct through-space manner. By synthesizing hetero-coupled binaphthalene derivatives

BN1-2 and **BN1-3**, constituted of oligothiophenes of different electron-richness, we have successfully expanded this concept. The emission spectrum of **BN1-3** shows a full quenching of the fluorescence as a result of charge transfer. Hyper-Rayleigh scattering experiments unambiguously reveal a significant enhancement of the second-order hyperpolarizability β resulting from a direct through-space charge transfer interaction between the p-type and the n-type oligomer. By the best of our knowledge, these experimental HRS values are the first published in the context of a direct through-space charge transfer interaction between a p-type and a n-type conjugated oligomer.

Acknowledgment: We are grateful to the Katholieke Universiteit Leuven (GOA), the Fund for Scientific Research (FWO-Vlaanderen). D. C. is a doctoral fellow of the IWT and G. K. and I. A. are postdoctoral fellows of the Fund for Scientific Research (FWO-Vlaanderen).

Supporting Information Available. Detailed ^{1}H-spectra of all the synthesized (bi)naphthalene derivatives, NOESY-spectrum of **BN2-2**, cyclic voltammograms of all (bi)naphthalene compounds, UV-vis and CD spectra of the chemical oxidation experiment on **BN2-2** and a UV-vis superposition spectrum of **BN1-3**. This material is available free of charge via the Internet at http://pubs.acs.org.

References:

(1) (a) Mishra, A.; Ma, C.-Q.; Bäuerle, P. *Chem. Rev.* **2009**, *109*, 1141 and references therein. (b) Hoeben, F. J. M.; Jonkheijm, P.; Meijer, E. W.; Schenning, A. P. H. J. *Chem. Rev.* **2005**, *105*, 14911 and references therein.

(2) Hunter, C. A.; Sanders, J. K. M. *J. Am. Chem. Soc.* **1990**, *112*, 5525.

(3) (a) Cornil, J.; Santos, D. A. D.; Crispin, X.; Silbey, R.; Brédas, J.-L. *J. Am. Chem. Soc.* **1998**, *120*, 1289. (b) Langeveld-Voss, B. M. W.; Beljonne, D.; Shuai, Z.; Janssen, R. A. J.; Meskers, S. C. J.; Meijer, E. W.; Brédas, J.-L. *Adv. Mater.* **1998**, *10*, 1343.

(4) (a) Brédas, J.-L.; Street, G. B. *Acc. Chem. Res.* **1985**, *18*, 309. (b) Heeger, A. J.; Kivelson, S.; Schrieffer, J. R.; Su, W. P. *Rev. Mod. Phys.* **1998**, *60*, 781.

(5) (a) Kaikawa, T.; Takimiya, K.; Aso, Y.; Otsubo, T. *Org. Lett.* **2000**, *2*, 4197. (b) Satou, T.; Sakai, T.; Kaikawa, T.; Takimiya, K.; Otsubo, T.; Aso, Y. *Org. Lett.* **2004**, *6*, 997. (c) Sakai, T.; Satou, T.; Kaikawa, T.; Takimiya, K.; Otsubo, T.; Aso, Y. *J. Am. Chem. Soc.* **2005**, *127*, 8082.

(6) Knoblock, K. M.; Silvestri, C. J.; Collard, D. M. *J. Am. Chem. Soc.* **2006**, *128*, 13680.

(7) (a) Song, C.; Swager, T. M. *Org. Lett.* **2008**, *10*, 3575. (b) Takita, R.; Song, C.; Swager, T. M. *Org. Lett.* **2008**, *10*, 5003.

(8) Cornelis, D.; Peeters, H.; Zrig, S.; Andrioletti, B.; Rose, E.; Verbiest, T.; Koeckelbergs, G. *Chem. Mater.* **2008**, *20*, 2133.

(9) Cornelis, D.; Verbiest, T.; Koeckelberghs, G. *Chem. Eur. J.* **2010**, *16*, 10963.

(10) Wang, S.; Bazan, G. C. *Chem. Phys. Lett.* **2001**, *333*, 437.

(11) (a) Zyss, J.; Ledoux, I.; Volkov, S.; Chernyak, V.; Mukamel, S.; Bartholomew, G. P.; Bazan, G. C. *J. Am. Chem. Soc.* **2000**, *122*, 11956. (b) Bartholomew, G. P.; Bazan, G.C. *J. Am. Chem. Soc.* **2002**, *124*, 5183.

(12) (a) Di Bella, S.; Ratner, M. A.; Marks, T. J. *J. Am. Chem. Soc.* **1992**, *114*, 5842. (b) Di Bella, S. ; Fragalá, I. L.; Ratner, M. A.; Marks, T. J. *J. Am. Chem. Soc.* **1993**, *115*, 682.

(13) Bao, D.; Millare B.; Xia, W.; Steyer, B. G.; Gerasimenko, A. A.; Ferreira, A.; Contreras, A.; Vullev, V. I. *J. Phys. Chem. A* **2009**, *113*, 1259.

(14) Olbrechts, G.; Strobbe, R.; Clays, K.; Persoons, A. *Rev. Sci. Instrum.* **1998**, *69*, 2233.

(15) (a) Ôi, S.; Matsuzaka, Y.; Yamashita, J.; Miyano, S. *Bull. Chem. Soc. Jpn.* **1989**, *62*, 956. (b) Furutani, T.; Hatsuda, M.; Imashiro, R.; Seki, M. *Tetrahedron: Asymmetry* **1999**, *10*, 4763.

(16) Bedworth, P. V.; Cai, Y.; Jen, A.; Marder, S. R. *J. Org. Chem.* **1996**, *61*, 2242.

(17) Hou, J.; Yang, C.; Li, Y. *Synth. Met.* **2005**, *153*, 93.

(18) Rathore, R.; Kumar, A. S.; Lindeman, S. V.; Kochi, J. K. *J. Org. Chem.* **1998**, *63*, 5847.

(19) (a) Seth, J.; Palaniappan, V.; Wagner, R. W.; Johnson, T. E.; Lindsey, J. S.; Bocian, D. F. *J. Am. Chem. Soc.* **1996**, *118*, 11194. (b) Wilson, T. M.; Tauber, M. J.; Wasielewski, M. R. *J. Am. Chem. Soc.* **2009**, *131*, 8952. (c) Wilson, T. M.; Hori, T.; Yoon, M.-C.; Aratani, N.; Osuka, A.; Kim, D.; Wasielewski, M. R. *J. Am. Chem. Soc.* **2010**, *132*, 1383.

(20) Malessa, M.; Heck, J.; Kopf, J.; Garcia, M. H. *Eur. J. Inorg. Chem.* **2006**, *4*, 1667.

(21) Hendrickx, E.; Vinckier, A.; Clays, K.; Persoons, A. *J. Phys. Chem.* **1996**, *100*, 19672.

(22) Zyss, J.; Ledoux, I. *Chem. Rev*., **1994**, *94*, 77.

(23) (a) Oudar, J. L.; Chemla, D. S. *J. Phys. Chem.* **1977**, *66*, 2664. (b) Wang, C. H. *J. Phys. Chem.* **2000**, *112*, 1917.

(24) β_{HRS} of **N1**, **N2** and **N3** are 430±30, 530±75 and 427±30 10^{-30} esu, respectively. However, since the symmetry of the model compounds and the BNs is significantly different and different resonant enhancement are present, the β_{HRS}-values cannot be compared. The depolarization ratios are 1.5-1.6.

(25) Interrante, L. V.; Hampden-Smith M. J., Eds. *Chemistry of Advanced Materials: an Overview*; Wiley VCH, Inc.: New York, 1997.

for Table of contents only

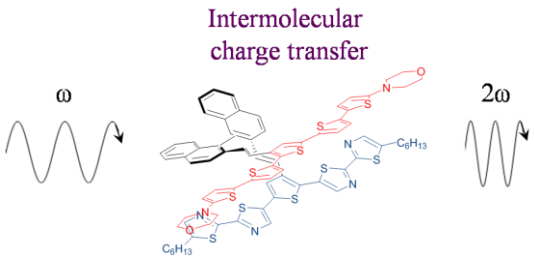
Intermolecular
charge transfer
ω
2ω